Dislocation-governed current-transport mechanism in (Ni/Au)–AlGaN/AlN/GaN heterostructures

Engin Arslan,[1,a] Şemsettin Altındal,[2] Süleyman Özçelik,[2] and Ekmel Ozbay[3]
[1]*Nanotechnology Research Center-NANOTAM, Bilkent University, 06800 Ankara, Turkey*
[2]*Department of Physics, Faculty of Science and Arts, Gazi University, Teknikokullar, 06500 Ankara, Turkey*
[3]*Department of Physics, Department of Electrical and Electronics Engineering, and Nanotechnology Research Center-NANOTAM, Bilkent University, 06800 Ankara, Turkey*

(Received 31 July 2008; accepted 4 December 2008; published online 22 January 2009)

The current-transport mechanisms in $(Ni/Au)-Al_{0,22}Ga_{0,78}N/AlN/GaN$ heterostructures were studied by using temperature dependent forward-bias current-voltage (*I-V*) characteristics in the temperature range of 80–410 K. In order to determine the current mechanisms for $(Ni/Au)-Al_{0,22}Ga_{0,78}N/AlN/GaN$ heterostructures, we fitted the experimental *I-V* data to the analytical expressions given for the current-transport mechanisms in a wide range of applied biases and at different temperatures. The contributions of thermionic-emission, generation-recombination, tunneling, leakage currents that are caused by inhomogeneities, and defects at the metal-semiconductor interface current mechanisms were all taken into account. The best fitting results were obtained for the tunneling current mechanism. On the other hand, we did not observe sufficient agreement between the experimental data and the other current mechanisms. The temperature dependencies of the tunneling saturation current (I_t) and tunneling parameters (E_0) were obtained from fitting results. We observed a weak temperature dependence of the saturation current and the absence of the temperature dependence of the tunneling parameters in this temperature range. The results indicate that in the temperature range of 80–410 K, the mechanism of charge transport in the $(Ni/Au)-Al_{0.22}Ga_{0.78}N/AlN/GaN$ heterostructure is performed by tunneling among those dislocations intersecting the space charge region. The dislocation density (*D*) that was calculated from the *I-V* characteristics, according to a model of tunneling along the dislocation line, gives the value of 0.24×10^{7} cm^{-2}. This value is close in magnitude to the dislocation density that was obtained from the x-ray diffraction measurements. © *2009 American Institute of Physics*.
[DOI: 10.1063/1.3068202]

I. INTRODUCTION

The transport properties of GaN and its alloys are attracting increasing interest due to the potential application of these materials for solar-blind photodetectors and high mobility transistors.[1–3] Because of the large energy band gap, the applications of $Al_xGa_{1-x}N$ are extensive, such as for visible-blind ultraviolet (UV) detectors, laser diodes, and short-wave light-emitting diodes.[4] High-quality AlGaN/GaN heterostructures have been shown to contain two-dimensional electron gas (2DEG), which has attracted special interest due to its potential applications in high mobility transistors operating at high power and high temperature levels.[5,6]

The device structures are usually grown on highly lattice-mismatched substrates, such as sapphire,[7] SiC,[8] or Si.[3,9] It still remains difficult to obtain a high-quality GaN epilayer because of the large lattice mismatch and large difference in the thermal expansion coefficients between the GaN film, sapphire, and SiC substrate. This fact causes a high level of in-plane stress and threading dislocation density (DD) generation, as grown by metal-organic chemical vapor deposition (MOCVD) in the GaN epitaxial layer.[7–9] These dislocations affect the performance reliability of the device.[1,2] Furthermore, it is well known that GaN usually has a high DD, much more than those in Si and GaAs semiconductors. If there exist many defects near the surface region, the electrons can easy go through the barrier by/via defect-assisted tunneling, thus greatly enhancing the tunneling probability. It is well established that the crystal qualities of Si and GaAs are far superior to that of GaN. For Schottky barriers on Si and GaAs with a doping concentration of $\sim10^{16}$ cm^{-3}, tunneling does not play a role in the current-transport mechanisms.

The current-transport mechanism in these devices such as metal semiconductor (MS), metal-insulator semiconductor (MIS), and solar cells are dependent on various parameters such as the process of surface preparation, formation of insulator layer between the metal and semiconductor, barrier height inhomogenity, impurity concentration of a semiconductor, density of interface states or defects, series resistance (R_s) of a device, device temperature, and bias voltage. In these devices, a number of carrier transport mechanisms such as quantum mechanical tunneling, thermionic emission (TE), thermionic field emission (TFE), minority carrier injection, recombination generation, and multistep tunneling compete, and usually, one of them may dominate over the others in a certain temperature and voltage regions. However, a simul-

[a]Author to whom correspondence should be addressed. Tel.: +90-312-2901971. FAX: +90-312-2901015. Electronic mail: engina@bilkent.edu.tr.

taneous contribution from two or more mechanisms could also be possible. Among them, TFE is important at low temperatures and high doping concentration levels. Voltage-proportional leakage currents frequently alter the current-voltage (*I-V*) relationship especially at lower bias voltage levels. These leakage currents are usually expressed by the addition of a term $(V\text{-}IR_s)/R_{sh}$ to the total current due to series resistance (R_s) and shunt resistance (R_{sh}) of device. More recently, experimental results have been shown for MS, MIS, and solar cells.[10–14] Very interesting studies among these were presented by Kar *et al.*[10] and Cao *et al.*,[11] where the results indicated the likelihood of a primary current-transport mechanism being multistep tunneling and defect-assisted tunneling instead of TE, respectively. Evstropov *et al.*[12,13] and Balyaev *et al.*[14] showed that the current flow in the III–V heterojunctions is generally governed by multistep tunneling with the involvement of dislocations even at room temperature. They demonstrated that an excess tunnel current can be attributed to dislocations. A model of tunneling through a space charge region along a dislocation line (tube) is suggested.[12]

Analysis of the current-voltage (*I-V*) characteristics of the MS, MIS, and solar cells measured only at room temperature does not provide detailed information about the current-conduction process and the nature of the barrier formed at the metal/semiconductor interface. On the other hand, the forward bias *I-V* characteristics at a wide temperature range enable us to understand the different aspects of the current-conduction mechanism and barrier formation. Therefore, the main aim of this study is to investigate the current-conduction mechanisms in AlGaN/AlN/GaN heterostructures with a high dislocation compared with the literature in a wide temperature range (80–410 K).

II. EXPERIMENTAL PROCEDURE

The $Al_xGa_{1-x}N/AlN/GaN$ ($x=0.22$) heterostructures were fabricated on (0001) on a double-polished 2 –in. diameter (0001), in which sapphire (Al_2O_3) substrates were grown in a low pressure MOCVD reactor (Aixtron 200/4 HT-S) by using trimethylgallium, trimethylaluminum, and ammonia as Ga, Al, and N precursors, respectively. Prior to the epitaxial growth, Al_2O_3 substrate was annealed at 1100 °C for 10 min in order to remove surface contamination. The buffer structures consisted of a 15 nm thick, low-temperature (650 °C) AlN nucleation layer, and high temperature (1150 °C) 420 nm AlN templates. A 1.5 μm nominally undoped GaN layer was grown on an AlN template layer at 1050 °C, followed by a 2 nm thick high temperature AlN (1150 °C) barrier layer. The AlN barrier layer was used to reduce the alloy disorder scattering by minimizing the wave function penetration from the 2DEG channel into the $Al_xGa_{1-x}N$ layer.[15] After the deposition of these layers, a 23 nm thick undoped $Al_{0.22}Ga_{0.78}N$ layer was grown on an AlN layer at 1050 °C. Finally, a 5 nm thick GaN cap layer growth was carried out at a temperature of 1085 °C and a pressure of 50 mbars.

Since the sapphire substrate is insulating, the Ohmic and Schottky/rectifier contacts were made bottom and top of the sample, respectively, in the high coating system at about 10^{-7} Torr. The Ohmic contacts were formed as a square van de Pauw shape and the Schottky contacts formed as 1 mm diameter circular dots (Fig. 1). Prior to Ohmic contact formation, the samples were cleaned. The samples are cleaned with acetone in an ultrasonic bath. Then, a sample was treated with boiling isopropyl alcohol for 5 min and rinsed in de-ionized (DI) water having 18 MΩ resistivity. After cleaning, the samples were dipped in a solution of HCl/H_2O (1:2) for 30 s in order to remove the surface oxides, and then rinsed in DI water again for a prolonged period. Ti/Al/Ni/Au (17.5/175/40/80 nm) metals were thermally evaporated on the sample and were annealed at 850 °C for 30 s in N_2 ambient in order to form the Ohmic contact. Schottky contacts were formed by Ni/Au (40/80 nm) evaporation.

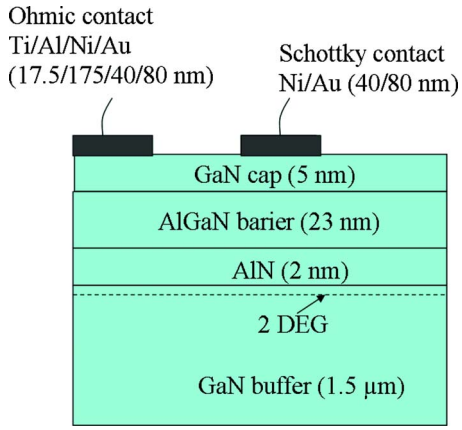

FIG. 1. (Color online) Schematic of the $Al_{0.22}Ga_{0.78}N/AlN/GaN$ heterostructure and a view of the Ohmic contact and Schottky contact on the structures.

The crystalline quality (DD) of the samples of the samples was examined by high-resolution x-ray diffraction (HRXRD). The x-ray diffraction was performed by using a Bruker D-8 high-resolution diffractometer system, delivering Cu Kα1 (1.540 Å) radiation. The current-voltage (*I-V*) measurements were performed by the use of a Keithley 2400 sourcemeter in the temperature range of 80–410 K using a temperature controlled Janes vpf-475 cryostat, which enables us to make measurements in the temperature range of 77–450 K. The sample temperature was continually monitored by using a copper-constant thermocouple close to the sample and measured with a Keithley model 199 dmm/scanner and a Lake Shore model 321 autotuning temperature controller with sensitivity better than ±0.1 K.

III. RESULTS AND DISCUSSION

In the present study, the $Al_{0.22}Ga_{0.78}N/AlN/GaN$ heterostructures were grown on sapphire with two steps exhibited high DDs.[3,7] The DD of the sample was investigated by the methods of high-resolution diffractometry. The DDs in the $Al_{0.22}Ga_{0.78}N/AlN/GaN$ heterostructures can be taken as equal to the DDs in the GaN layers.[3] There are three main types of dislocations that are present in the GaN epitaxial layers.[16,17] The pure edge dislocation with Burgers vector $b=\frac{1}{3}\langle 11\bar{2}0\rangle$ ($\langle a\rangle$), the pure screw dislocation with Burgers vec-

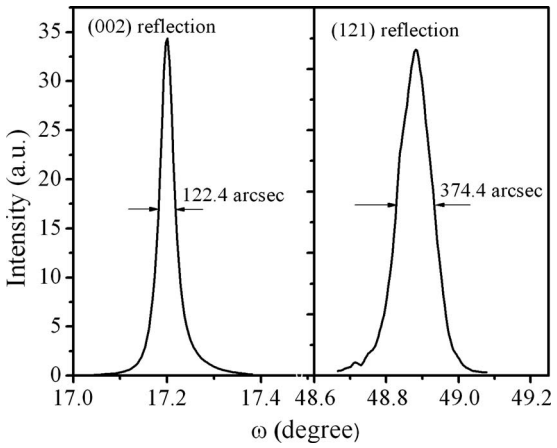

FIG. 2. The x-ray rocking curves for (002) and (121) reflections of the GaN epilayer.

tor $b=\langle 0001\rangle$ ($\langle c\rangle$), and the mixed dislocation with $b=\frac{1}{3}\langle 11\bar{2}3\rangle$ ($\langle \mathbf{c}+\mathbf{a}\rangle$). These DDs of GaN can be determined from the following equations:[16]

$$D_{\text{screw}}=\frac{\beta^2_{(002)}}{9b^2_{\text{screw}}},\quad D_{\text{edge}}=\frac{\beta^2_{(121)}}{9b^2_{\text{edge}}}, \tag{1}$$

$$D_{\text{dis}}=D_{\text{screw}}+D_{\text{edge}}, \tag{2}$$

where D_{screw} is the screw DD, D_{edge} is the edge DD, β is the full width at half maximum (FWHM) of the measured XRD rocking curves, and b is the Burgers vector length ($b_{\text{screw}}=0.5185$ nm, $b_{\text{edge}}=0.3189$ nm). The measured XRD rocking curves for (002) and (121) reflections are shown in Fig. 2. The FWHM values measured for (002) and (121) reflections are 122.4 and 374.4 arc sec, respectively. By using Eqs. (1) and (2), we calculated the values for screw, edge, and total DDs as 1.45×10^7, $2,41\times10^8$, and 2.55×10^8 cm^{-2}, respectively.

In order to correctly interpret the current-transport mechanisms in the $(\text{Ni/Au})-\text{Al}_{0,22}\text{Ga}_{0,78}\text{N/AlN/GaN}$ heterostructures, we considered the contribution of TE current and various other current-transport mechanisms. Thus, the generation recombination, tunneling, and leak currents caused by the inhomogenities and defects at the M/S interface were taken into full account. In general, the relationship between the applied-bias voltage ($V\geq 3kT/q$) and the current of the Schottky diodes, based on the TE theory, is given by[18]

$$I_{\text{thermionic}}=I_0\exp\left[\frac{q(V-IR_s)}{nkT}\right]\left\{1-\exp\left[\frac{-q(V-IR_s)}{kT}\right]\right\}, \tag{3}$$

where I_0 is the saturation current derived from the straight-line intercept of $\ln I$ at zero bias and is given by

$$I_0=AA^*T^2\exp\left(-\frac{q\Phi_{b0}}{kT}\right), \tag{4}$$

where A is the rectifier contact area, A^* is the effective Richardson constant ($32.09\ \text{A/cm}^2\ \text{K}^2$ for undoped $\text{Al}_{0,22}\text{In}_{0,78}\text{N}$),[19] T is the absolute temperature in kelvins, q is the electron charge, Φ_{B0} is the zero-bias apparent Schottky barrier height, n is the ideality factor, V is the applied-bias voltage, and IR_s term is the voltage drop across the R_s of structure. The generation-recombination current can be described by the relation[20]

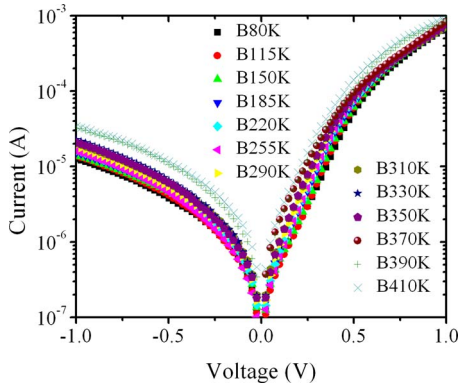

FIG. 3. (Color online) Experimental forward and reverse bias semilogarithmic current-voltage characteristics of a $(\text{Ni/Au})-\text{Al}_{0.22}\text{Ga}_{0.78}\text{N/AlN/GaN}$ heterostructure at different temperatures.

$$I_{g-r}=I_{gr}\left\{\exp\left[\frac{q(V-IR_s)}{2kT}\right]-1\right\} \tag{5}$$

with

$$I_{gr}=\frac{qn_iW_d}{2\tau}, \tag{6}$$

where I_{gr} is the generation-recombination saturation current, n_i is the intrinsic carrier concentration, W_d is the depletion layer width, and τ is the effective carrier lifetime. The tunneling current through the barrier is given by[18]

$$I_{\text{tunnel}}=I_t\left\{\exp\left[\frac{q(V-IR_s)}{E_0}\right]-1\right\}, \tag{7}$$

where I_t is the tunneling saturation current and E_0 is the tunneling parameter. E_0 can be defined as[21–23]

$$E_0=E_{00}\coth\left(\frac{E_{00}}{kT}\right), \tag{8}$$

where E_{00} is the characteristic tunneling energy that is related to the tunnel effect transmission probability. It is evident that the mechanism of charge transport is tunnel, which is indicated by a weak temperature dependence of the saturation current. In addition, voltage-proportional leakage currents frequently alter the current-voltage (I-V) relationship at lower bias voltage levels and can be expressed as[21]

$$I_{\text{leakage}}=\frac{V-IR_s}{R_{\text{sh}}}. \tag{9}$$

Thus, the total current of device can be expressed as

$$I_{\text{total}}=I_{\text{thermionic}}+I_{g-r}+I_{\text{tunnel}}+I_{\text{leakage}}. \tag{10}$$

Figure 3 shows a set of semilogarithmic forward bias I-V characteristics of a $(\text{Ni/Au})-\text{Al}_{0.22}\text{Ga}_{0.78}\text{N/AlN/GaN}$ heterostructure that was measured in the temperature range of 80–410 K. As shown in Fig. 3, the forward bias of structure

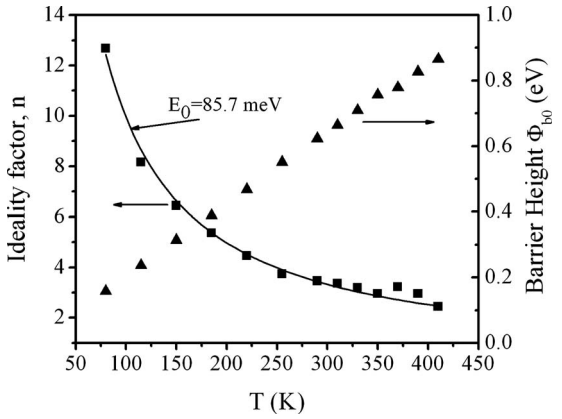

FIG. 4. The zero-bias barrier height Φ_{b0} and the ideality factor n of a $(Ni/Au)-Al_{0.22}Ga_{0.78}N/AlN/GaN$ heterostructure obtained from the forward bias I-V data at various temperatures. The straight line is the least-squares fit of Eq. (8) to the ideality factor (n) data.

current is an exponential function of the applied-bias voltage in the intermediate voltage regime ($0.1 \leq V \leq 0.6$ V). It is clear that over a broad range ($10^{-6}-10^{-4}$ A) of forward current, the behavior is exponential and beyond that ($I \geq 10^{-4}$ A) the plots deviate from this behavior due to the effect of series resistance (R_s). Moreover, these plots are parallel over a forward-current range of $10^{-6}-10^{-4}$ A. To interpret the observed electrical characteristics of an $(Ni/Au)-Al_{0.22}Ga_{0.78}N/AlN/GaN$ heterostructure, Riben and Feucht[23] developed a multistep recombination-tunneling model. This model successfully explains the functional dependence of the forward current on applied voltage and temperature. The model, assuming a staircase path that consists of a series of tunneling transitions between trapping levels in the diode space charge region coupled with a series of vertical steps where the carrier loses energy by transferring from one level to another. However, such a process is only possible if the concentration of the trapping levels is sufficiently high. In this model, the carrier tunneling between the defect levels increases the probability of tunneling through the entire barrier.

The temperature dependent values of zero-bias barrier height (Φ_{b0}) and ideality factor (n), as calculated from the semilogarithmic forward bias $\ln I$ versus V characteristics, are shown in Fig. 4 and Table I. As can be seen in Fig. 4 and Table I, the values of Φ_{b0} increase with increasing temperature, in which there is a positive coefficient that is contrary to the negative dependence measurements by Crowell and Rideout[24] in silicon Shottky diodes and Mead and Spitzer[25] in InAs and InSb, which closely follows the charge in forbidden energy band gap (E_g) with temperature. This contradiction is possible due to Eq. (4), which is not representative of the reverse saturation current of our samples implying that the current transport is not the TE.

For the tunneling dominated current-transport equation (7), the slope of the $\ln I$ versus V plot ($q/E_0=q/nkT$) is essentially temperature independent and is called a voltage factor or tunneling constant. In addition, at a constant bias voltage, $\ln I$ is more of a linear function of temperature than an inverse temperature. According to the tunneling model, which was developed for Schottky barriers, the band bending works as a barrier for carriers tunneling into interface states or dislocations, where various traps may be involved in multitunneling steps.[23] Thermally activated carriers make (stepwise) tunneling into the interface states. The values of slope $\ln I$ versus V plots at different temperatures with the corresponding values of the ideality factor [obtained from Eq. (3)] are shown in Table I and Fig. 4. As can be seen in Table I, the n values changes from 12.68 (at 80 K) to 2.44 (at 410 K). However, the slope and nT values remain almost unchanged over the same temperature range with an average of 11.35 V^{-1} and 1025 K, respectively. The high value of n has been attributed to several effects such as interface states, tunneling currents in the high dislocations,[12–14] image force lowering of the Schottky barrier in the high electric field at a MS interface, and generation currents within the space-charge region.[18] The TFE mechanism can be ruled out in this region, since nT is more or less constant in the measured temperature range. Apart from discussing the main carrier transport mechanisms, the ideality factor is further analyzed

TABLE I. Temperature dependent values of various parameters determined from the forward bias I-V characteristics of $(Ni/Au)-Al_{0.22}Ga_{0.78}N/AlN/GaN$ heterostructure. In the eighth and ninth columns, the values of tunneling saturation current (I_t) and tunneling parameters (E_0), obtained by least-squares fit of tunneling current mechanism [Eq. (7)] to the measured I-V data, are listed.

T (K)	I_0 x10^{-7} A	Slope (A V^{-1})	n	nT (K)	E_0 (eV)	Φ_{b0} (eV)	E_0 (eV)	I_t x10^{-7} A
80	1.84	11.43	12.68	1014.59	0.087	0.16	0.092	3.14
115	1.44	12.36	8.16	938.33	0.081	0.24	0.093	3.19
150	1.79	12.00	6.44	966.04	0.083	0.31	0.096	3.64
185	2.52	11.68	5.37	992.73	0.086	0.39	0.095	4.27
220	2.56	11.79	4.47	982.63	0.085	0.47	0.096	4.51
255	2.30	12.15	3.74	954.53	0.082	0.55	0.096	4.45
290	3.46	11.55	3.46	1003.46	0.086	0.63	0.094	5.00
310	4.26	11.13	3.36	1041.96	0.090	0.66	0.096	5.53
330	4.37	10.99	3.19	1054.58	0.091	0.71	0.096	6.08
350	4.26	11.19	2.96	1035.69	0.089	0.76	0.098	6.38
370	9.28	9.70	3.23	1194.78	0.103	0.78	0.096	6.62
390	8.68	10.06	2.95	1152.02	0.099	0.83	0.096	6.66
410	1.07	11.57	2.44	1002.09	0.086	0.86	0.097	7.03

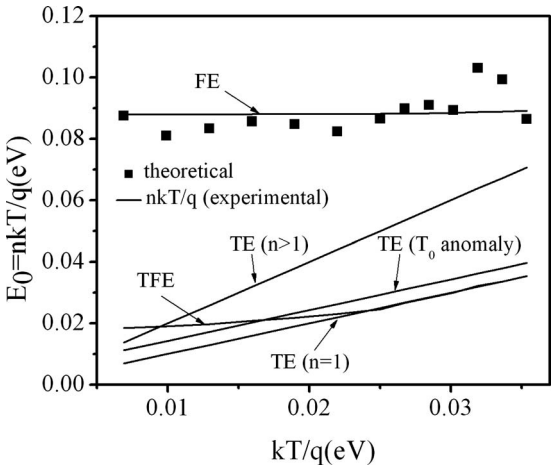

FIG. 5. Experimentally and theoretically found tunneling current parameter $E_0(nkT/q)$ vs kT/q for $(Ni/Au)-Al_{0.22}Ga_{0.78}N/AlN/GaN$ heterostructure.

by plotting nkT/q against kT/q as shown in Fig. 5, which shows the experimental and theoretical results of these plots. If the FE dominates, then the E_0 data will lay on a straight line as can be seen in Fig. 5. In this case, E_0 is independent of the temperature and E_0 is very close to the E_{00} values.[26] In our study, the average value of E_0 was found to be 88.5 meV, which is very close to the 85.7 meV value of E_{00} that was obtained from the fitting of Eq. (8) to the $n(T)$ data (Fig. 4).

In order to determine the true current-transport mechanisms for $(Ni/Au)-Al_{0,22}Ga_{0,78}N/AlN/GaN$ heterostructures, by taking the I_{te}, I_{gr}, I_t, the tunneling parameter E_0 and the R_s and R_{sh} as adjustable fit parameters, we fit the experimental I-V data to the analytical expressions given for the current-transport mechanisms in a wide range of applied biases and at different temperatures. A standard software package was utilized for the curve fitting. As shown in Fig. 6, there is an excellent agreement between the measured I-V data and the current-transport expressions for the tunneling mechanism at all temperature range. However, there is no good fit between the measured I-V data and the analytic expression given for TE, generation recombination, or the leakage current mechanism at all the temperatures (Fig. 6). The tunneling saturation current I_t and E_0 values, as determined from the fits of the tunneling current expression to the measured I-V data set, are summarized in the eighth and ninth columns of Table I. Similar results have been reported in the literature.[11–14,26–29]

The temperature dependences of I_t and E_0 are shown in Fig. 7. The results indicate that in the temperature range of 80–410 K, the mechanism of charge transport in the $(Ni/Au)-Al_{0.22}Ga_{0.78}N/AlN/GaN$ heterostructure is tunneling, which is demonstrated by a weak temperature dependence of the saturation current and the absence of the temperature dependence of the tunneling parameters in this temperature range. The I-V behavior of the tunneling current in the barrier structures fabricated based on degenerate semiconductors (Schottky diodes, p-n heterojunctions) can be expressed by Eq. (7) according to the dislocation model of the tunneling current, and the tunneling saturation current (I_t) can be represented by the equation of the form[12,14]

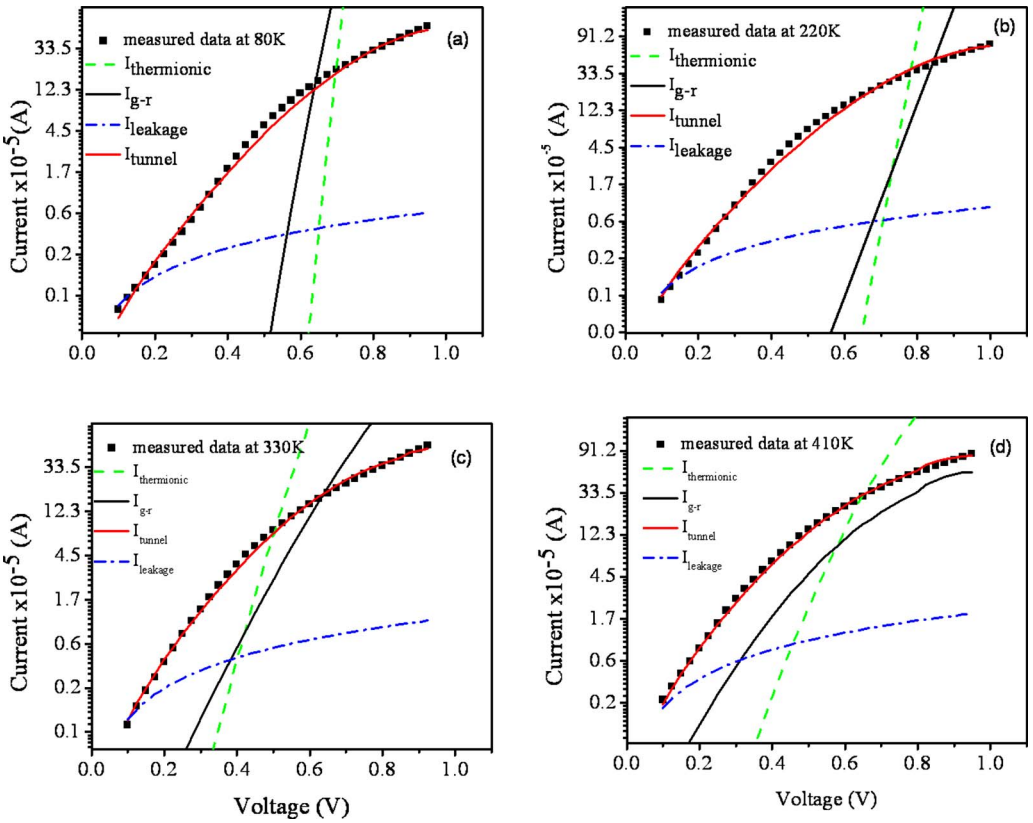

FIG. 6. (Color online) The least-squares fits of the TE [Eq. (3)], generation recombination [Eq. (5)], tunneling [Eq. (7)], and leakage current [Eq. (9)] equation to the I-V data measured at (a) 80 K, (b) 250 K, (c) 330 K, and (d) 410 K.

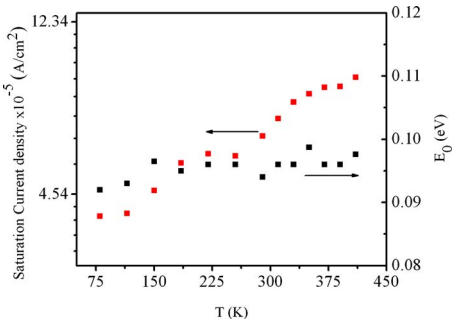

FIG. 7. (Color online) Temperature dependence of tunneling saturation current I_t and tunneling parameter E_0, which were calculated from the tunneling current equation fits to measured *I-V* data.

$$I_t = qD\nu_D \exp(-qV_K/E_0), \tag{11}$$

where D is the DD, $\nu_D \approx 1.68\times10^{13}$ s^{-1} is the Debye frequency[30] for $Al_{0.22}Ga_{0.78}N$ layer and $qV_K=\Phi_B-\mu_n$ is the diffusion potential for the Schottky barrier diode (SBD). In this equation, Φ_B is the height of the SBD, $\mu_n \cong kT\ln(N_C/N_D)$ is the chemical potential, N_c is the effective density of states in the conduction band,[18] N_D is the concentration of the ionized donors in the AlGaN barrier layer, and $E_0=nkT$ is the tunneling parameter.

By using the model equation (11) and determined I_t and E_0 from the measured *I-V* characteristic as well as knowing $V_K(0)$, which is the expression for the DD that can be given as[12–14]

$$D_{\text{dis}} = \frac{I_t(0)}{q\nu_D}\exp\left[\frac{qV_K(0)}{E_0}\right], \tag{12}$$

where $I_t(0)$ and $E_0(0)$ can be obtained by the extrapolation to zero of the absolute temperature of the temperature dependences of $I_t(0)$ and $E_0(0)$. The value of $qV_K(0)$ can be calculated from the empirical dependence of Φ_B on the band gap E_g in GaN (because in our study Schottky diodes were done on GaN cap layers), $\Phi_B \approx \frac{1}{3}E_g^{\text{GaN}}$,[14]

$$qV_K(0) = \Phi_B(0) - \mu_n(0) \cong \tfrac{1}{3}E_g^{\text{GaN}}(0) - \mu_n(0). \tag{13}$$

By using $I_t(0)$, $E_0(0)$, $qV_K(0)$, and $E_g(0)=3.47$ eV values for GaN, the DD can be calculated by Eq. (12). In addition, this case was supported by the experimental values of the height of the Schottky barrier that was formed on the GaN layers by pure metals Ni, Pt, Ir,[31] and Au.[32] In the present study, we calculated the DD by using $I_t(0)=2.31\times10^{-5}$ A/cm^2, $E_0(0)=0.092$ eV, and $qV_K(0)=1.15$ eV values. We obtained 0.24×10^7 cm^{-2}, which are near the results that were obtained from the XRD measurements. The DDs measured from XRD are 1.45×10^7, $2,41\times10^8$, and 2.55×10^8 cm^{-2} for the total dislocations, screw-, and edge-type DD, respectively. These DDs are consistent with the values given for GaN epitaxial films in the literature.[3,4,9] Analysis of the forward bias *I-V* data indicated that the predominant current mechanism of the $Al_{0.22}Ga_{0.78}N/AlN/GaN$ heterostructure with high DDs in the intermediate bias voltage region that was investigated in this study was a dislocation-governed current-transport mechanism rather than the other current-transport mechanisms.

IV. CONCLUSIONS

The current-transport mechanism across $(Ni/Au)-Al_{0,22}Ga_{0,78}N/AlN/GaN$ heterostructures was carried out by using temperature dependent forward-bias current-voltage (*I-V*) characteristics in the temperature range of 80–410 K. The best fitting results were obtained for the tunneling current equation. However, we did not obtain a fit for the other current mechanisms. We did not observe sufficient agreement between the experimental data and the other current mechanisms. The tunneling saturation current (I_t) and tunneling parameter E_0 were determined from the fitting process. The typical features of a tunnel saturation current (I_t) temperature dependence were weak and E_0 was nearly independent of the temperature. These results show that the charge transport mechanism in the temperature range of 80–410 K in the forward-biased $(Ni/Au)-Al_{0,22}Ga_{0,78}N/AlN/GaN$ heterostructures was performed by the tunneling mechanism among the dislocations intersecting the space charge region.

ACKNOWLEDGMENTS

This work is supported by the European Union under the projects EU-METAMORPHOSE, EU-PHOREMOST, EU-PHOME, and EU-ECONAM, and TUBITAK under the Project Nos. 105E066, 105A005, 106E198, 106A017, and 107A012. One of the authors (E.O.) also acknowledges partial support from the Turkish Academy of Sciences.

[1] S. N. Mohammad, A. Salvador, and H. Morkoç, Proc. IEEE **83**, 1420 (1996).
[2] L. Shen, S. Heikman, B. Moran, R. Coffie, N.-Q. Zhang, D. Buttari, I. P. Smorchkova, S. Keller, S. P. DenBaars, and U. K. Mishra, IEEE Electron Device Lett. **22**, 457 (2001).
[3] E. Arslan, S. Bütün, S. B. Lisesivdin, M. Kasap, S. Ozcelik, and E. Ozbay, J. Appl. Phys. **103**, 103701 (2008).
[4] S. Nakamura, M. Senoh, S. Nagahama, N. Iwasa, T. Yamada, T. H. Kiyoku, Y. Sugimoto, T. Kozaki, H. Umemoto, M. Sano, and K. Chocho, Appl. Phys. Lett. **72**, 1687 (1998).
[5] L. Hsu and W. Walukiewicz, Phys. Rev. B **56**, 1520 (1997).
[6] N. Biyikli, Ü. Özgür, X. Ni, Y. Fu, H. Morkoç, and Ç. Kurdak, J. Appl. Phys. **100**, 103702 (2006).
[7] H. Yu, D. Caliskan, and E. Ozbay, J. Appl. Phys. **100**, 033501 (2006).
[8] R. Gaska, J. W. Yang, A. Osinsky, Q. Chen, M. Asif Khan, A. O. Orlov, G. L. Snider, and M. S. Shur, Appl. Phys. Lett. **72**, 707 (1998).
[9] A. Dadgar, C. Hums, A. Diez, J. Bläsing, and A. Krost, J. Cryst. Growth **297**, 279 (2006).
[10] S. Kar, K. M. Panchal, S. Bhattacharya, and S. Varma, IEEE Trans. Electron Devices **29**, 1839 (1982).
[11] X. A. Cao, S. F. LeBoeuf, K. H. Kim, P. M. Sandvik, E. B. Stokes, A. Ebong, D. Walker, J. Kretchmer, J. Y. Lin, and H. X. Jiang, Solid-State Electron.. **46**, 2291 (2002).
[12] V. V. Evstropov, M. Dzhumaeva, Yu. V. Zhilyaev, N. Nazarov, A. A. Sitnikova, and L. M. Fedorov, Fiz. Tekh. Poluprovodn. (S.-Peterburg) **34**, 1357 (2000) [Semiconductors **34**, 1305 (2000)].
[13] V. V. Evstropov, Yu. V. Zhilyaev, M. Dzhumaeva, and N. Nazarov, Fiz. Tekh. Poluprovodn. (S.-Peterburg) **31**, 152 (1997) [Semiconductors **31**, 115 (1997)].
[14] A. E. Belyaev, N. S. Boltovets, V. N. Ivanov, V. P. Klad'ko, R. V. Konakova, Ya. Ya. Kudrik, A. V. Kuchuk, V. V. Milenin, Yu. N. Sveshnikov, and V. N. Sheremet, Semiconductors **42**, 689 (2008).
[15] M. N. Gurusinghe, S. K. Davidsson, and T. G. Andersson, Phys. Rev. B **72**, 045316 (2005).
[16] T. Metzger, R. H¨oppler, E. Born, O. Ambacher, M. Stutzmann, R. Stommer, M. Schuster, H. Gobel, S. Christiansen, M. Albrecht, and H. P. Strunk, Philos. Mag. A **77**, 1013 (1998).
[17] E. Arslan, M. K. Ozturk, A. Teke, S. Ozcelik, and E. Ozbay, J. Phys. D **41**,

155317 (2008).
[18]S. M. Sze, *Physics of Semiconductor Devices* (Wiley, New York, 1981).
[19]A. J. Sierakowski and L. F. Eastman, J. Appl. Phys. **86**, 3398 (1999).
[20]A. Y. C. Yu and E. H. Snow, J. Appl. Phys. **39**, 3008 (1968).
[21]D. Donoval, M. Barus, and M. Zdimal, Solid-State Electron.. **34**, 1365 (1991).
[22]H. Bayhan and A. Sertap Kavasoğlu, Solid-State Electron. **49**, 991 (2005).
[23]A. R. Riben and D. L. Feucht, Int. J. Electron. **20**, 583 (1966).
[24]C. R. Crowell and V. L. Rideout, Solid-State Electron. **12**, 89 (1969).
[25]C. A. Mead and W. G. Spitzer, Phys. Rev. **134**, A713 (1964).
[26]A. N. Saxena, Surf. Sci. **13**, 151 (1969).
[27]J. J. Marchand and K. Truong, J. Appl. Phys. **54**, 7034 (1983).
[28]S. Özdemir and Ş. Aştındal, Sol. Energy Mater. Sol. Cells **32**, 115 (1994).
[29]S. Ashok, P. P. Sharma, and S. J. Fonash, IEEE Trans. Electron Devices **27**, 725 (1980).
[30]H. Morkoc, *Handbook of Nitride Semiconductors and Devices* (Wiley-VCH, New York, 2008), Vol. 1.
[31]V. Kumar, D. Selvanathan, A. Kuliev, S. Kim, J. Flynn, and I. Adesida, Electron. Lett. **39**, 747 (2003).
[32]E. Monroy, F. Calle, R. Ranchal, T. Palacios, M. Verd'u, F. J. S'anchez, M. T. Montojo, M. Eickhoff, F. Omn′es, Z. Bougrioua, and I. Moerman, Semicond. Sci. Technol. **17**, L47 (2002).